ISSN 1063-7710, Acoustical Physics, 2016, Vol. 62, No. 6, pp. 672–680. © Pleiades Publishing, Ltd., 2016.

CLASSICAL PROBLEMS
OF LINEAR ACOUSTICS AND WAVE THEORY

An Extension of the Transfer Matrix Method to Analyzing Acoustic Resonators with Gradually Varying Cross-Sectional Area[1]

Qi Min, Wan-Quan He, Quan-Biao Wang, and Jia-Jin Tian

Department of Physics, Honghe University, Mengzi, Yunnan 661100, China

e-mail: minq7@163.com

Received September 10, 2015

Abstract—The transfer matrix method was used to analyze the acoustical properties of stepped acoustic resonator in the previous paper. The present paper extends the application of the transfer matrix method to analyzing acoustic resonators with gradually varying cross-sectional area. The transfer matrices and the resonant conditions are derived for acoustic resonators with four different kinds of gradually varying geometric shape: tapered, trigonometric, exponential and hyperbolic. Based on the derived transfer matrices, the acoustic properties of these resonators are derived, including the resonant frequency, phase and radiation impedance. Compared with other analytical methods based on the wave equation and boundary conditions, the transfer matrix method is simple to implement and convenient for computation.

Keywords: transfer matrix, stepped acoustic resonator, gradually varying acoustic resonator

DOI: 10.1134/S1063771016060117

1. INTRODUCTION

This paper is a sequel to the previous paper [1], in which the transfer matrix method was applied in the analysis of stepped acoustic resonator, and the merits of this method in calculating the acoustic properties of stepped acoustic resonator were revealed. Compared with other analytical methods based on the wave equation and boundary conditions, the transfer matrix method is simple to implement and convenient for computation. Based on the derived transfer matrix method, important acoustic properties of stepped acoustic resonator, such as the resonant frequency, phase and radiation impedance, were calculated quite efficiently.

A stepped acoustic resonator is composed of two or more sub-tubes with different diameters and has one or more abrupt variations of cross-sectional area in the axial direction. With such a simple geometric construction, the stepped acoustic resonator can be manufactured easily and cheaply. However, with the increase of sound pressure level, especially when the sound field becomes nonlinear, much more energy loss occurs at the location of abrupt variation of cross-sectional area compared with that in a smooth transition with gradually varying cross-sectional area. Hence a sub-tube with gradually varying cross-sectional area is often inserted between two sub-tubes with different diameters to reduce energy loss, and the stepped acoustic resonator is transformed into a stepped acoustic resonator with gradually varying cross-section along the axial direction [1–5].

In practice, four types of gradually varying geometric shape are commonly used: tapered, trigonometric, exponential and hyperbolic [6, 7]. Among these four types of variation, the tapered variation is the easiest type for manufacture. Even though, compared with stepped acoustic resonators with abrupt cross-section, the manufacturing of all types of gradually varying resonators is time-consuming, especially for large-size resonators. Nonetheless, in order to obtain standing waves with long wavelength and large amplitude, a stepped acoustic resonator with gradually varying cross-sectional area in the axial direction is a good choice [2–5].

This paper extends the transfer matrix method to analyzing four types of acoustic resonators with gradually varying cross-sectional areas. For brevity, the four types of variation are labeled as “tap”, “tri”, “exp”, and “hyp” in the following figures, equations and tables. This paper is organized as follows: firstly, the mathematical representations of each type of shape variation and the sound field in each types of sub-tube are introduced in section 2; next, the transfer matrix and the resonant condition for each type of acoustic resonator are derived in section 3; then, based on the derived transfer matrix, the acoustic properties of each type of acoustic resonator are calculated, such as the resonant frequency, phase and radiation impedance in section 4 and 5; finally, conclusions are given in section 6.

2. GRADUALLY VARYING SHAPE AND SOUND FIELD

2.1. Gradually Varying Geometric Shape

Four types of gradually varying geometric shape: taper, trigonometric function, exponential form and hyperbola, are shown in Fig. 1. The cross-sectional

[1] The article is published in the original.

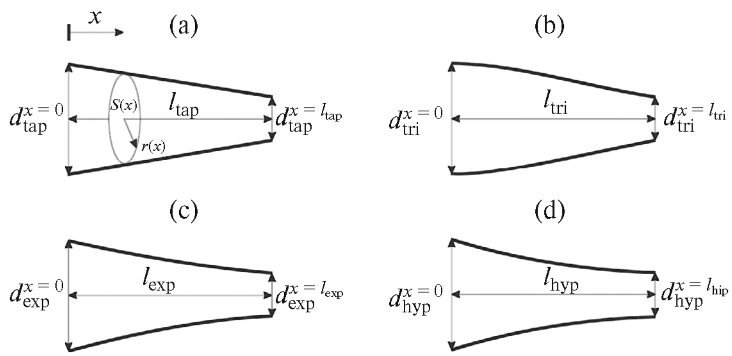

Fig. 1. Gradual geometric shapes: (a) tapered, (b) trigonometric, (c) exponential, and (d) hyperbolic.

area $S(x)$ at location x in the axial direction of any gradual shape is mathematically described by [6, 8]

$$S(x) = Af(x,\delta), \tag{1}$$

where A is an undetermined constant and δ is the shape factor. The radius of the cross sectional area at x is $r(x)$ and the diameter is $d(x)$. The specific cross-sectional area $S(x)$ and shape factor δ for the four types of variation under consideration are shown in Table 1.

2.2. Sound Field

The sound field $p(x,t)$ in an acoustic sub-tube with cross-sectional area $S(x)$ is governed by the Webster horn equation [8]

$$\frac{\partial^2 p(x,t)}{\partial x^2} + \left[\frac{\partial \ln S(x)}{\partial x}\right]\frac{\partial p(x,t)}{\partial x} = \frac{1}{c_0^2}\frac{\partial^2 p(x,t)}{\partial t^2}. \tag{2}$$

Let ω be the angle frequency and $p(x,t) = p(x)e^{j\omega t}$, and we have

$$p(x,t) = p_{Ai}\frac{1}{B(x)}e^{j(\omega t - Kx)} + p_{Ar}\frac{1}{B(x)}e^{j(\omega t + Kx)}, \tag{3}$$

where the subscript Ai in p_{Ai} represents the forward traveling wave and Ar in p_{Ar} represents the backward traveling wave; $B(x)$and K are undetermined functions and satisfy

$$\begin{cases} B(x) = 1/r(x), \\ K^2 = k^2 - r(x)''/r(x), \end{cases} \tag{4}$$

where k is the wave vector. Consequently, the particle velocity is

$$\begin{aligned} v(x,t) = &-\frac{p_{Ai}}{\rho_0}\int \frac{\partial\left[e^{j(\omega t - Kx)}/B(x)\right]}{\partial x}dt \\ &-\frac{p_{Ar}}{\rho_0}\int \frac{\partial\left[e^{j(\omega t - Kx)}/B(x)\right]}{\partial x}dt. \end{aligned} \tag{5}$$

Equations (3) and (5) give the general expression for the acoustic pressure $p(x,t)$ and particle velocity $v(x,t)$ in a gradually varying acoustic sub-tube, respectively. For each kind of variation, the expressions of acoustic pressure $p(x,t)$ and particle velocity $v(x,t)$ are then derived:

Tapered

$$\begin{aligned} p_{\rm tap}(x,t) = &\ p_{Ai}^{\rm tap}(1-\delta_{\rm tap}x)^{-1}e^{j(\omega t - kx)} \\ &+ p_{Ar}^{\rm tap}(1-\delta_{\rm tap}x)^{-1}e^{j(\omega t + kx)}, \end{aligned} \tag{6a}$$

$$\begin{aligned} &v_{\rm tap}(x,t) \\ &= -p_{Ai}^{\rm tap}\frac{\left[\delta_{\rm tap}(1-\delta_{\rm tap}x)^{-2} - jk(1-\delta_{\rm tap}x)^{-1}\right]}{jk\rho_0 c_0}e^{j(\omega t - kx)} \\ &\quad - p_{Ar}^{\rm tap}\frac{\left[\delta_{\rm tap}(1-\delta_{\rm tap}x)^{-2} + jk(1-\delta_{\rm tap}x)^{-1}\right]}{jk\rho_0 c_0}e^{j(\omega t + kx)}. \end{aligned} \tag{6b}$$

Table 1. Shape factor δ and cross-sectional area $S(x)$ of four kinds of gradually varying shape

	Tapered	Trigonometric	Exponential	Hyperbolic
δ	$\dfrac{d_{\rm tap}^{x=l_{\rm tap}} - d_{\rm tap}^{x=0}}{d_{\rm tap}^{x=l_{\rm tap}}l_{\rm tap}}$	$\dfrac{1}{l_{\rm tri}}\arccos\left(\dfrac{d_{\rm tri}^{x=0}}{d_{\rm tri}^{x=l_{\rm tri}}}\right)$	$\dfrac{2}{l_{\rm exp}}\ln\left(\dfrac{d_{\rm exp}^{x=0}}{d_{\rm exp}^{x=l_{\rm exp}}}\right)$	$\dfrac{1}{l_{\rm hyp}}\cosh^{-1}\left(\dfrac{d_{\rm hyp}^{x=0}}{d_{\rm hyp}^{x=l_{\rm hyp}}}\right)$
$S(x)$	$\pi d_{\rm tap}^{x=l_{\rm tap}}(1-\delta_{\rm tap}x)^2$	$\pi d_{\rm tri}^{x=l_{\rm tri}}\cos^2(\delta_{\rm tri}x)$	$\pi d_{\rm exp}^{x=l_{\rm exp}}e^{\delta_{\rm exp}x}$	$\pi d_{\rm hyp}^{x=l_{\rm hyp}}\cosh^2(\delta_{\rm hyp}x)$

Trigonometric

$$p_{\text{tri}}(x,t) = p_{Ai}^{\text{tri}}\cos^{-1}(\delta_{\text{tri}}x)e^{j(\omega t - k_{\text{tri}}x)} + p_{Ar}^{\text{tri}}\cos^{-1}(\delta_{\text{tri}}x)e^{j(\omega t + k_{\text{tri}}x)}, \tag{7a}$$

$$v_{\text{tri}}(x,t) = -p_{Ai}^{\text{tri}}\frac{\left[\cos^{-2}(\delta_{\text{tri}}x)\sin(\delta_{\text{tri}}x)\delta_{\text{tri}} - (jk_{\text{tri}})\cos^{-1}(\delta_{\text{tri}}x)\right]}{jk\rho_0 c_0}e^{j(\omega t - k_{\text{tri}}x)} - p_{Ar}^{\text{tri}}\frac{\left[\cos^{-2}(\delta_{\text{tri}}x)\sin(\delta_{\text{tri}}x)\delta_{\text{tri}} + (jk_{\text{tri}})\cos^{-1}(\delta_{\text{tri}}x)\right]}{jk\rho_0 c_0}e^{j(\omega t + k_{\text{tri}}x)}, \tag{7b}$$

where $k_{\text{tri}} = \sqrt{k^2 + \delta_{\text{tri}}^2}$.

Exponential

$$p_{\exp}(x,t) = p_{Ai}^{\exp}e^{-\frac{\delta_{\exp}}{2}x}e^{j(\omega t - k_{\exp}x)} + p_{Ar}^{\exp}e^{-\frac{\delta_{\exp}}{2}x}e^{j(\omega t + k_{\exp}x)}, \tag{8a}$$

$$v_{\exp}(x,t) = p_{Ai}^{\exp}\frac{\delta_{\exp}/2 + jk_{\exp}}{jk\rho_0 c_0}e^{-\frac{\delta_{\exp}}{2}x}e^{j(\omega t - k_{\exp}x)} + p_{Ar}^{\exp}\frac{\delta_{\exp}/2 - jk_{\exp}}{jk\rho_0 c_0}e^{-\frac{\delta_{\exp}}{2}x}e^{j(\omega t + k_{\exp}x)}, \tag{8b}$$

where $k_{\exp} = \sqrt{k^2 - (\delta_{\exp}/2)^2}$.

Hyperbolic

$$p_{\text{hyp}}(x,t) = p_{Ai}^{\text{hyp}}\{\cosh[\delta_{\text{hyp}}(l_{\text{hyp}} - x)]\}^{-1}e^{j(\omega t - k_{\text{hyp}}x)} + p_{Ar}^{\text{hyp}}\{\cosh[\delta_{\text{hyp}}(l_{\text{hyp}} - x)]\}^{-1}e^{j(\omega t + k_{\text{hyp}}x)}, \tag{9a}$$

$$v_{\text{hyp}}(x,t) = -p_{Ai}^{\text{hyp}}\frac{\{\cosh[\delta_{\text{hyp}}(l_{\text{hyp}} - x)]\}^{-2}\sinh[\delta_{\text{hyp}}(l_{\text{hyp}} - x)]\delta_{\text{hyp}} - jk_{\text{hyp}}\{\cosh[\delta_{\text{hyp}}(l_{\text{hyp}} - x)]\}^{-1}}{jk\rho_0 c_0}e^{j(\omega t - k_{\text{hyp}}x)} - p_{Ar}^{\text{hyp}}\frac{\{\cosh[\delta_{\text{hyp}}(l_{\text{hyp}} - x)]\}^{-2}\sinh[\delta_{\text{hyp}}(l_{\text{hyp}} - x)]\delta_{\text{hyp}} + (jk_{\text{hyp}})\{\cosh[\delta_{\text{hyp}}(l_{\text{hyp}} - x)]\}^{-1}}{jk\rho_0 c_0}e^{j(\omega t + k_{\text{hyp}}x)}, \tag{9b}$$

where $k_{\text{hyp}} = \sqrt{k^2 - \delta_{\text{hyp}}^2}$.

3. TRANSFER MATRIX AND RESONANT CONDITION

3.1. Transfer Matrix

Following Eq. (3) and Eq. (5), the acoustic pressure and particle velocity at two ports, i.e. the input port at $x = 0$ and the output port at $x = l$, in a gradually varying acoustic sub-tube can be given by: $x = 0$

$$p(0) = M(0)p_{Ai} + m(0)p_{Ar}, \tag{10a}$$

$$v(0) = N(0)p_{Ai} + n(0)p_{Ar}; \tag{10b}$$

$x = l$

$$p(l) = M(l)e^{-jKl}e^{-\alpha l}p_{Ai} + m(l)e^{jKl}e^{\alpha l}p_{Ar}, \tag{11a}$$

$$v(l) = N(l)e^{-jKl}e^{-\alpha l}p_{Ai} + n(l)e^{jKl}e^{\alpha l}p_{Ar}; \tag{11b}$$

where M, m, N and n are undetermined coefficients. As a result, the transfer matrix that connects the two ports becomes [1–5, 9]

$$\begin{bmatrix} p(l) \\ v(l) \end{bmatrix} = \begin{bmatrix} F_{p11}e^{-jKl}e^{-\alpha l} + F_{p12}e^{jKl}e^{\alpha l} & -\left(F_{p21}e^{-jKl}e^{-\alpha l} + F_{p22}e^{jKl}e^{\alpha l}\right) \\ F_{v11}e^{-jKl}e^{-\alpha l} + F_{v12}e^{jKl}e^{\alpha l} & -\left(F_{v21}e^{-jKl}e^{-\alpha l} + F_{v22}e^{jKl}e^{\alpha l}\right) \end{bmatrix} \begin{bmatrix} p(0) \\ v(0) \end{bmatrix}, \tag{12}$$

where the attenuation coefficient $\alpha = 6.36\times10^{-4}\sqrt{f}/d_{\text{ave}}$ and $d_{\text{ave}} = (d_{x=0} + d_{x=l})/2$ [1–5, 10]. For a standing-wave resonator, $M(0) = m(0)$ and $M(l) = m(l)$, so the coefficients in matrix (12) are

$$F_{p11} = \frac{M(l)M(0)^{-1}}{1 - N(0)n(0)^{-1}},\; F_{p12} = \frac{M(l)M(0)^{-1}}{1 - n(0)N(0)^{-1}},$$

$$F_{p21} = \frac{M(l)}{n(0) - N(0)},\; F_{p22} = \frac{M(l)}{N(0) - n(0)},$$

and

$$F_{v11} = \frac{N(l)m(0)^{-1}}{1 - N(0)n(0)^{-1}},\; F_{v12} = \frac{n(l)M(0)^{-1}}{1 - n(0)N(0)^{-1}},$$

$$F_{v21} = \frac{N(l)n(0)^{-1}}{1 - N(0)n(0)^{-1}},\; F_{v22} = \frac{n(l)N(0)^{-1}}{1 - n(0)N(0)^{-1}}.$$

Based upon the matrix in Eq. (12), the transfer matrix for each kind of area variation is derived:

Tapered

$$\begin{bmatrix} p_{\text{tap}}(l_{\text{tap}}) \\ v_{\text{tap}}(l_{\text{tap}}) \end{bmatrix} = \begin{bmatrix} -\left(F_{Aip}F_p e^{-jkl_{\text{tap}}}e^{-\alpha_{\text{tap}}l_{\text{tap}}} + F_{Arp}F_p e^{jkl_{\text{tap}}}e^{\alpha_{\text{tap}}l_{\text{tap}}}\right) & F_{Aiv}F_p e^{-jkl_{\text{tap}}}e^{-\alpha_{\text{tap}}l_{\text{tap}}} + F_{Arv}F_p e^{jkl_{\text{tap}}}e^{\alpha_{\text{tap}}l_{\text{tap}}} \\ -\left(F_{Aip}F_{vi} e^{-jkl_{\text{tap}}}e^{-\alpha_{\text{tap}}l_{\text{tap}}} + F_{Arp}F_{vr} e^{jkl_{\text{tap}}}e^{\alpha_{\text{tap}}l_{\text{tap}}}\right) & F_{Aiv}F_{vi} e^{-jkl_{\text{tap}}}e^{-\alpha_{\text{tap}}l_{\text{tap}}} + F_{Arv}F_{vr} e^{jkl_{\text{tap}}}e^{\alpha_{\text{tap}}l_{\text{tap}}} \end{bmatrix} \begin{bmatrix} p_{\text{tap}}(0) \\ v_{\text{tap}}(0) \end{bmatrix}, \tag{13}$$

where

$$F_{Aip} = \left[\frac{(-\delta_{\text{tap}} + jk)}{(-\delta_{\text{tap}} - jk)} - 1\right]^{-1},\; F_{Aiv} = \frac{jk\rho_0 c_0}{(-\delta_{\text{tap}} - jk)}F_{Aip},$$

$$F_{Arp} = \left[\frac{(-\delta_{\text{tap}} - jk)}{(-\delta_{\text{tap}} + jk)} - 1\right]^{-1},\; F_{Arv} = \frac{jk\rho_0 c_0}{(-\delta_{\text{tap}} + jk)}F_{Arp},$$

$$F_p = (1 - \delta_{\text{tap}}l_{\text{tap}})^{-1},$$

$$F_{vi} = \frac{\left[-\delta_{\text{tap}}F_p^{\,2} + jkF_p\right]}{jk\rho_0 c_0},\; F_{vr} = \frac{\left[-\delta_{\text{tap}}F_p^{\,2} - jkF_p\right]}{jk\rho_0 c_0}.$$

Trigonometric

$$\begin{bmatrix} p_{\text{tri}}(l_{\text{tri}}) \\ v_{\text{tri}}(l_{\text{tri}}) \end{bmatrix} = \frac{1}{2}\begin{bmatrix} \left(F_p^{\text{tri}} e^{-jk_{\text{tri}}l_{\text{tri}}}e^{-\alpha_{\text{tri}}l_{\text{tri}}} + F_p^{\text{tri}} e^{jk_{\text{tri}}l_{\text{tri}}}e^{\alpha_{\text{tri}}l_{\text{tri}}}\right) & \left(F_{Av}F_p^{\text{tri}} e^{-jk_{\text{tri}}l_{\text{tri}}}e^{-\alpha_{\text{tri}}l_{\text{tri}}} - F_{Av}F_p^{\text{tri}} e^{jk_{\text{tri}}l_{\text{tri}}}e^{\alpha_{\text{tri}}l_{\text{tri}}}\right) \\ \left(F_{vi}^{\text{tri}} e^{-jk_{\text{tri}}l_{\text{tri}}}e^{-\alpha_{\text{tri}}l_{\text{tri}}} + \dfrac{F_{vr}^{\text{tri}}}{2} e^{jkl_{\text{tri}}}e^{\alpha_{\text{tri}}l_{\text{tri}}}\right) & \left(F_{Av}F_{vi}^{\text{tri}} e^{-jk_{\text{tri}}l_{\text{tri}}}e^{-\alpha_{\text{tri}}l_{\text{tri}}} - F_{Av}F_{vr}^{\text{tri}} e^{jk_{\text{tri}}l_{\text{tri}}}e^{\alpha_{\text{tri}}l_{\text{tri}}}\right) \end{bmatrix} \begin{bmatrix} p_{\text{tri}}(0) \\ v_{\text{tri}}(0) \end{bmatrix}, \tag{14}$$

where

$$F_{Av} = \frac{k\rho_0 c_0}{k_{\text{tri}}},\; F_p^{\text{tri}} = \frac{1}{\cos(\delta_{\text{tri}}l_{\text{tri}})},$$

$$F_{vi}^{\text{tri}} = -\frac{\left[\cos^{-2}(\delta_{\text{tri}}l_{\text{tri}})\sin(\delta_{\text{tri}}l_{\text{tri}})\delta_{\text{tri}} - (jk_{\text{tri}})\cos^{-1}(\delta_{\text{tri}}l_{\text{tri}})\right]}{jk\rho_0 c_0},$$

$$F_{vr}^{\text{tri}} = -\frac{\left[\cos^{-2}(\delta_{\text{tri}} l_{\text{tri}})\sin(\delta_{\text{tri}} l_{\text{tri}})\delta_{\text{tri}} + (jk_{\text{tri}})\cos^{-1}(\delta_{\text{tri}} l_{\text{tri}})\right]}{jk\rho_0 c_0}.$$

Exponential

$$\begin{bmatrix} p_{\exp}(l_{\exp}) \\ v_{\exp}(l_{\exp}) \end{bmatrix} = \begin{bmatrix} -\begin{pmatrix} F_{Ai}(F_{Ar}-F_{Ai})^{-1} e^{-\frac{\delta_{\exp}}{2} l_{\exp} - jk_{\exp} l_{\exp}} e^{-\alpha_{\exp} l_{\exp}} \\ + F_{Ar}(F_{Ai}-F_{Ar})^{-1} e^{-\frac{\delta_{\exp}}{2} l_{\exp} + jk_{\exp} l_{\exp}} e^{\alpha_{\exp} l_{\exp}} \end{pmatrix} & \begin{matrix} (F_{Ai}-F_{Ar})^{-1} e^{-\frac{\delta_{\exp}}{2} l_{\exp} - jk_{\exp} l_{\exp}} e^{-\alpha_{\exp} l_{\exp}} \\ + (F_{Ar}-F_{Ai})^{-1} e^{-\frac{\delta_{\exp}}{2} l_{\exp} + jk_{\exp} l_{\exp}} e^{\alpha_{\exp} l_{\exp}} \end{matrix} \\ -\begin{pmatrix} F_{Ai}^2(F_{Ar}-F_{Ai})^{-1} e^{-\frac{\delta_{\exp}}{2} l_{\exp} - jk_{\exp} l_{\exp}} e^{-\alpha_{\exp} l_{\exp}} \\ + F_{Ar}^2(F_{Ai}-F_{Ar})^{-1} e^{-\frac{\delta_{\exp}}{2} l_{\exp} + jk_{\exp} l_{\exp}} e^{\alpha_{\exp} l_{\exp}} \end{pmatrix} & \begin{matrix} F_{Ai}(F_{Ai}-F_{Ar})^{-1} e^{-\frac{\delta_{\exp}}{2} l_{\exp} - jk_{\exp} l_{\exp}} e^{-\alpha_{\exp} l_{\exp}} \\ + F_{Ar}(F_{Ar}-F_{Ai})^{-1} e^{-\frac{\delta_{\exp}}{2} l_{\exp} + jk_{\exp} l_{\exp}} e^{\alpha_{\exp} l_{\exp}} \end{matrix} \end{bmatrix} \begin{bmatrix} p_{\exp}(0) \\ v_{\exp}(0) \end{bmatrix}, \quad (15)$$

where

$$F_{Ai} = \frac{\left(\frac{\delta_{\exp}}{2} + jk_{\exp}\right)}{jk\rho_0 c_0}, \quad F_{Ar} = \frac{\left(\frac{\delta_{\exp}}{2} - jk_{\exp}\right)}{jk\rho_0 c_0}.$$

Hyperbolic

$$\begin{bmatrix} p_{\text{hyp}}(l_{\text{hyp}}) \\ v_{\text{hyp}}(l_{\text{hyp}}) \end{bmatrix} = \frac{1}{2}\begin{bmatrix} [\cosh(\delta_{\text{hyp}} l_{\text{hyp}})]^{-1}\begin{pmatrix} e^{-jk_{\text{hyp}} l_{\text{hyp}}} e^{-\alpha_{\text{hyp}} l_{\text{hyp}}} \\ + e^{jk_{\text{hyp}} l_{\text{hyp}}} e^{\alpha_{\text{hyp}} l_{\text{hyp}}} \end{pmatrix} & -[\cosh(\delta_{\text{hyp}} l_{\text{hyp}})]^{-1}\begin{pmatrix} \frac{1}{F_{vi}^{\text{hyp}}} e^{-jk_{\text{hyp}} l_{\text{hyp}}} e^{-\alpha_{\text{hyp}} l_{\text{hyp}}} \\ - \frac{1}{F_{vi}^{\text{hyp}}} e^{jk_{\text{hyp}} l_{\text{hyp}}} e^{\alpha_{\text{hyp}} l_{\text{hyp}}} \end{pmatrix} \\ -\begin{pmatrix} F_{vv} e^{-jk_{\text{hyp}} l_{\text{hyp}}} e^{-\alpha_{\text{hyp}} l_{\text{hyp}}} \\ + F_{vp}^{\text{hyp}} e^{jk_{\text{hyp}} l_{\text{hyp}}} e^{\alpha_{\text{hyp}} l_{\text{hyp}}} \end{pmatrix} & \begin{pmatrix} \frac{F_{vv}}{F_{vi}^{\text{hyp}}} e^{-jk_{\text{hyp}} l_{\text{hyp}}} e^{-\alpha_{\text{hyp}} l_{\text{hyp}}} \\ - \frac{F_{vp}^{\text{hyp}}}{F_{vi}^{\text{hyp}}} e^{jk_{\text{hyp}} l_{\text{hyp}}} e^{\alpha_{\text{hyp}} l_{\text{hyp}}} \end{pmatrix} \end{bmatrix} \begin{bmatrix} p_{\text{hyp}}(0) \\ v_{\text{hyp}}(0) \end{bmatrix}, \quad (16)$$

where

$$F_{vi}^{\text{hyp}} = \frac{k_{\text{hyp}}}{k\rho_0 c_0},$$

$$F_{vp}^{\text{hyp}} = \frac{[\cosh(\delta_{\text{hyp}} l_{\text{hyp}})]^{-2}[\sinh(\delta_{\text{hyp}} l_{\text{hyp}})]\delta_{\text{hyp}} - jk_{\text{hyp}}\cosh[(\delta_{\text{hyp}} l_{\text{hyp}})]^{-1}}{jk\rho_0 c_0},$$

$$F_{vv} = \frac{[\cosh(\delta_{\text{hyp}} l_{\text{hyp}})]^{-2}[\sinh(\delta_{\text{hyp}} l_{\text{hyp}})]\delta_{\text{hyp}} + jk_{\text{hyp}}\cosh[(\delta_{\text{hyp}} l_{\text{hyp}})]^{-1}}{jk\rho_0 c_0}.$$

3.2. Resonant Condition

Let the acoustic resource be mounted at the open end of the input port at $x = 0$. Since the output port at $x = l$ is a closed end, such a sub-tube is an acoustic resonator/standing-wave tube with gradually varying cross-sectional area. For a gradually varying acoustic resonator whose length is roughly odd times of a quarter of the wave length and without considerable acoustic attenuation, we have $p(0) = 0$ and $v(l) = 0$ in the transfer matrix Eq. (12) when the sound field is resonant. As a result, the resonant condition is [1, 5]

$$F_{v21} e^{-jKl} + F_{v22} e^{jKl} = 0. \quad (17)$$

Table 2. Resonant conditions for gradually varying acoustic resonators with length of about odd times of a quarter of the wavelength

Tapered	Trigonometric	Exponential	Hyperbolic
$\frac{\tan(kl_{tap})}{kl_{tap}} = \delta_{tap} l_{tap}$	$\tan(k_{tri} l_{tri}) = -\frac{k_{tri}}{\delta_{tri}} \cot(\delta_{tri} l_{tri})$	$\tan(k_{exp} l_{exp}) = \frac{2k_{exp}}{\delta_{exp}}$	$\cosh(\delta_{hyp} l_{hyp}) \tan(k_{hyp} l_{hyp}) = \frac{k_{hyp}}{\delta_{hyp}}$

The resonant condition calculated with Eq. (17) for each gradually varying acoustic resonator is given in Table 2. Since all the derived resonant conditions are transcendental equations, these acoustic resonators are dissonant. Hence, these gradually varying acoustic resonators could be used to obtain a high-amplitude acoustic standing-wave field [1–5].

4. TRANSFER FUNCTION AND PHASE

In this section, the transfer functions and phases of the four kinds of gradually varying acoustic resonator are computed numerically.

In the previous paper, the transfer function of sound pressure (SPTF) of a gradually varying acoustic resonator was defined as [1–5]

$$H = 20\log\left|\frac{p(l)}{p(0)}\right| = L(l) - L(0), \tag{18}$$

where $L(0)$ is the acoustic pressure at the input port ($x = 0$) and $L(l)$is that at the output port ($x = l$).

In the numerical simulation in this study, four gradually varying acoustic resonators are considered, which have the same diameter at the input port (49 mm) and the same diameter at the output port (15 mm), and they also have the same length (330 mm).

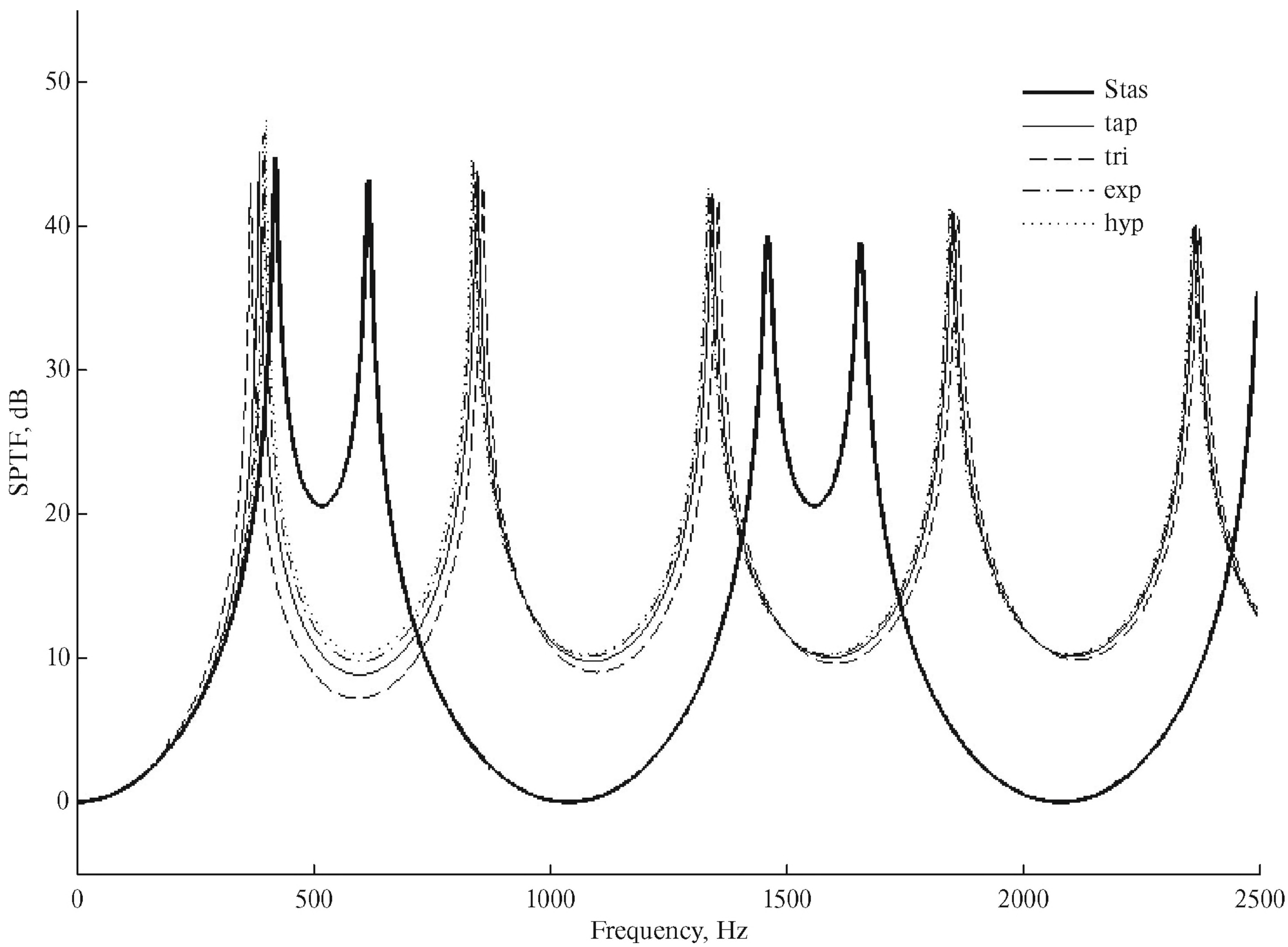

Fig. 2. Transfer function of sound pressure (SPTF) of gradually varying acoustic resonator and two-step resonator.

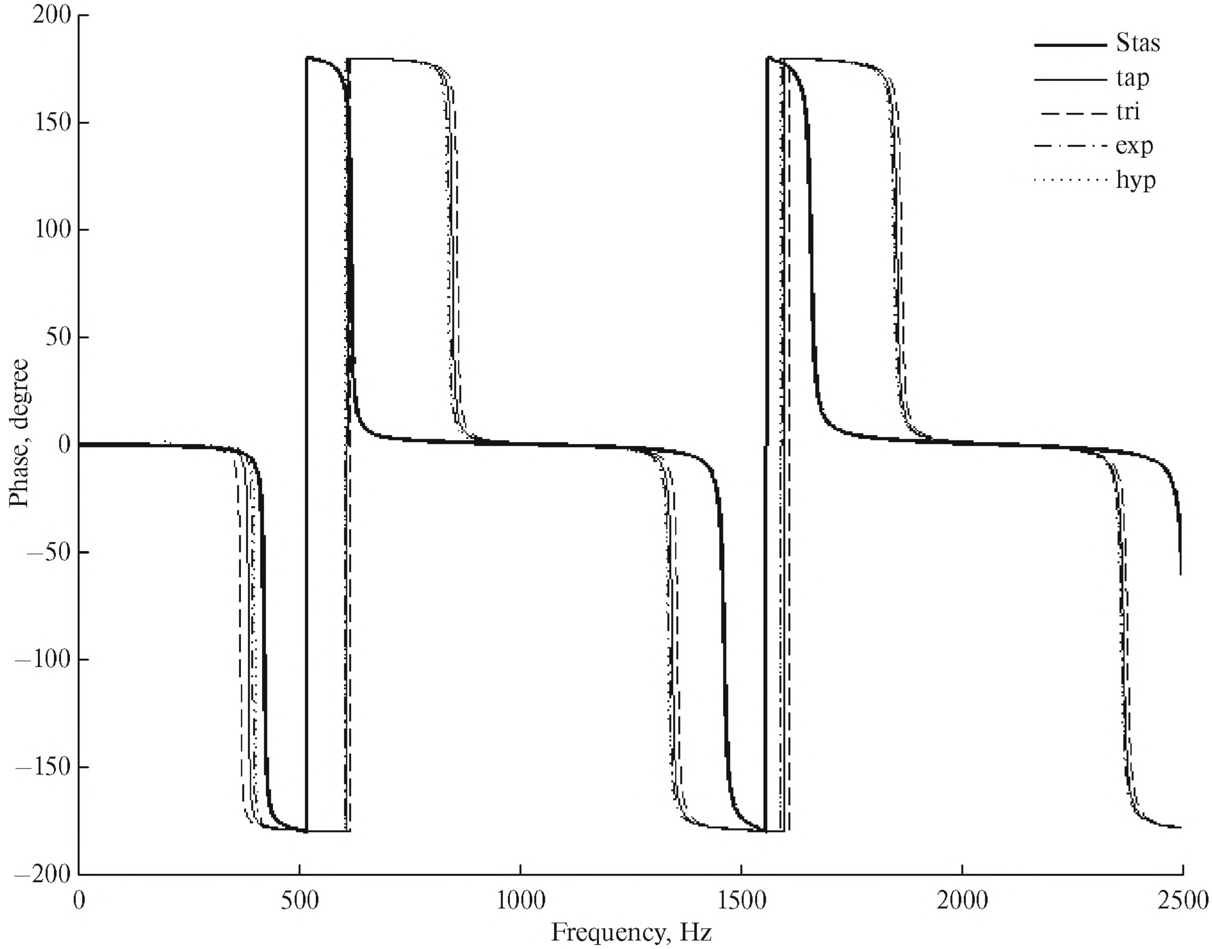

Fig. 3. Phase of gradually varying acoustic resonator and two-step resonator.

The transfer matrices in Eq. (14)–(16) are then used to calculate the transfer functions and phases of the four acoustic resonators with gradually varying shapes, and the results of the transfer functions are shown in Fig. 2 and the results of the phases are shown in Fig. 3. For comparison, the transfer function and the phase of a two-step acoustic resonator with abruptly varied cross-sectional area are also shown in Fig. 2 and Fig. 3, respectively. For brevity, the two-step acoustic resonator is labeled as Stas [1, 2]. The diameter of one sub-tube is 49 mm and that of the second sub-tube is 15 mm, corresponding to the size of the input port and the output port of the four simulated gradually varying acoustic resonators, respectively. Moreover, both sub-tubes have the same length (165 mm), so the total length of the two-step acoustic resonator (330 mm) is the same as the lengths of the four gradually varying acoustic resonators.

Figure 2 shows that, unlike the two-step acoustic resonator, the resonant frequencies of the four gradually varying acoustic resonators at the peaks and the valleys of SPTF do not distribute evenly in the frequency domain. All the four gradually varying acoustic resonators are dissonant: at peak resonant frequencies, the length of the resonator is about odd times of a quarter of the wavelength; at valley resonant frequencies, the length of the resonator is about even times of a quarter of the wavelength. In addition, for all resonators, the SPTF at the peak resonant frequency decreases with frequency, and for each resonator, the maximum SPTF located at the first peak resonant frequency exceeds 40 dB. Furthermore, for the two-step acoustic resonator, some of the SPTFs at the valley resonant frequencies are zero, but for the four gradually varying acoustic resonators, all the SPTFs at valley resonant frequencies are greater than zero.

Figure 3 shows that for all resonators, including the two-step acoustic resonator and the four gradually varying resonators, the absolute values of phase at the peak resonant frequencies are about 90°, and those at the valley resonant frequencies are about 0° or 180°.

In addition, an acoustic sub-tube with tapered shape and the simulated sizes is also manufactured, since this shape variation can be most easily machined among the four kinds of gradually varying acoustic

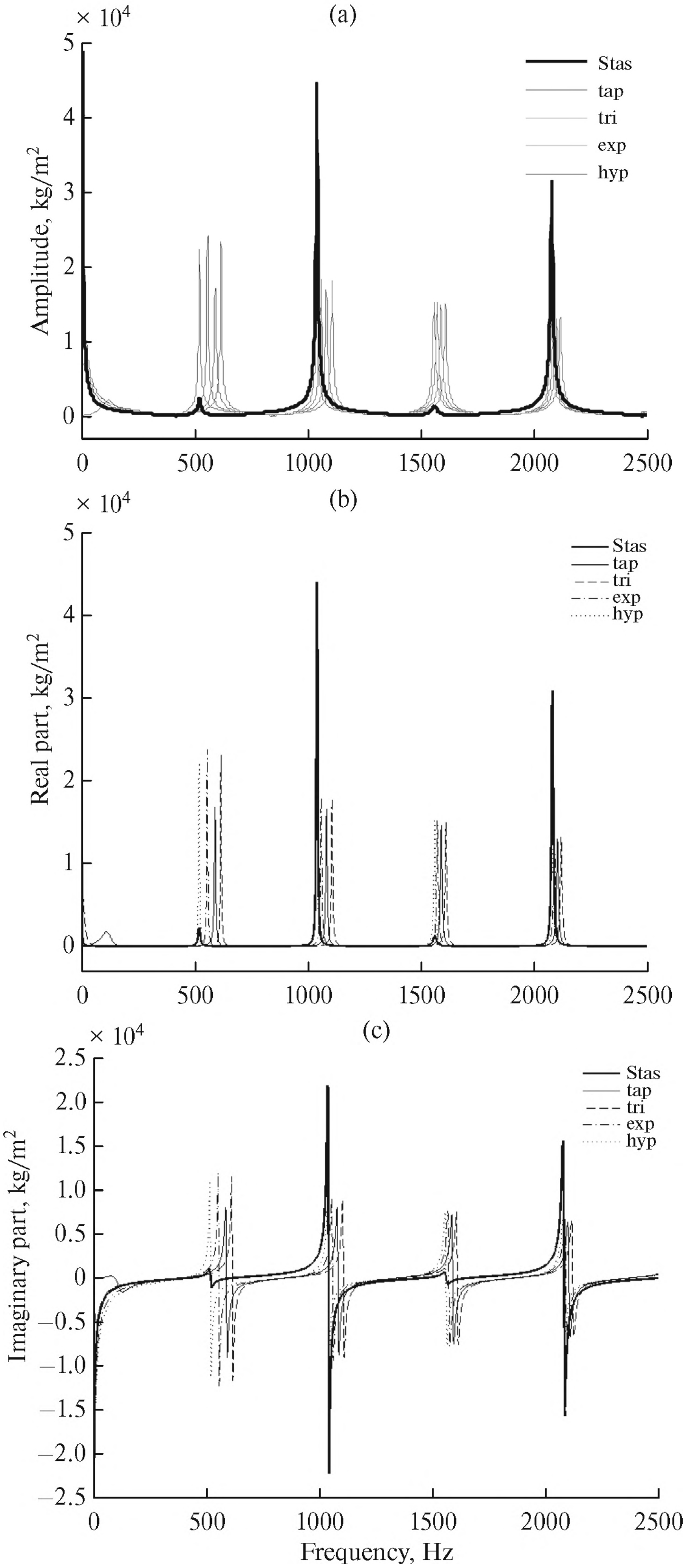

Fig. 4. Impedance of gradually varying acoustic resonator and two-step resonator: (a) amplitude, (b) real part and (c) imaginary part.

resonators. The simulated and measured acoustic properties of a stepped acoustic resonator formed by the sub-tube with tapered shape will be reported in the next paper.

5. IMPEDANCE

The radiation impedances at the input ports of the four gradually varying acoustic resonators and the two-step acoustic resonator are also calculated with the transfer matrixes in Eqs. (14)–(16), and the results are shown in Fig. 4.

Figure 4a shows that the amplitudes of radiation impedance at the valley resonant frequencies of the four gradually varying acoustic resonators decrease with frequency, but those of the two-step acoustic resonator display different behavior. The maximum amplitude exceeding 4×10^4 kg/m^2 is located at the second valley resonant frequency. However, the amplitudes at the peak resonant frequencies all approach zero for all resonators, including the four gradually varying resonators and the two-step acoustic resonator.

Figure 4b shows that for the four gradually varying resonators, the real parts of radiation impedances at the valley resonant frequencies also decrease with frequency, and the real parts of the radiation impedances of all resonators, including the two-step acoustic resonator, are very close to the corresponding amplitudes shown in Fig. 4a. Interestingly, the real parts of radiation impedance at the peak resonant frequencies of all acoustic resonators are zero.

Figure 4c shows that for each acoustic resonator, the absolute values of the imaginary parts of radiation impedances at the valley resonant frequencies are much smaller than both the amplitudes and the real parts of radiation impedances, but the imaginary parts of radiation impedances at the peak resonant frequencies are not zero.

6. CONCLUSIONS

The transfer matrix method was extended to analyze the acoustical properties of acoustic resonators with gradually varying cross-sectional areas in this paper. For each one of four kinds of gradually varying acoustic resonator: tapered, trigonometric, exponential and hyperbolic, the transfer matrix is first derived, and then the resonant condition is determined, along with other acoustic properties such as resonant frequencies and radiation impedance.

Numerical simulation of four acoustic resonators with gradually varying cross-sectional areas and a two-step resonator with abrupt variation in cross-sectional area shows that for each resonator, the transfer function in sound pressure and the resonant frequencies is unevenly distributed in the frequency domain, and the gradually varying acoustic resonators are dissonant.

For all resonators, the transfer functions at the peak resonant frequencies decrease with frequency; moreover, the absolute values of phase at the peak resonant frequencies are all about 90°, and those at the valley resonant frequencies are about 0° or 180°. However, the transfer functions at the valley resonant frequencies are all greater than zero for the four gradually varying acoustic resonators, but for the stepped resonator, the values at some valley resonant frequencies are zero.

The variation of radiation impedance at the input port shows similar pattern of variation of the transfer function of sound pressure. Both the amplitudes and the real parts of radiation impedances at the valley resonant frequencies decrease with frequency for each gradually varying acoustic resonator, but not for the two-step acoustic resonator. The real parts of radiation impedances at the peak resonant frequencies of all acoustic resonators are zero, but the imaginary parts of radiation impedances at the peak resonant frequencies are not zero.

ACKNOWLEDGMENTS

The research was supported by the National Natural Science Foundation of China (Grant no. 11364017).

REFERENCES

1. Q. Min, Q. Y. Zhang, J. J. Tian, Q. B. Wang, and W. Q. He, Acoust. Phys. **60**, 492 (2014).
2. Q. Min, Q. Y. Zhang, J. J. Tian, Q. B. Wang, and W. Q. He, Phys. Lett. A **377**, 99 (2012).
3. Q. Min, Y. Yin, X. D. Li, and K. Liu, Acta Acoust. **30**, 409 (2011).
4. Q. Min, F. Peng, Y. Yin, and K. Liu, Acta Acoust. **29**, 321 (2010).
5. Q. Min and K. Liu, Acta Phys. Sin. **60**, 024301 (2011) [in Chinese].
6. C. C. Lawrenson, B. Lipkens, T. S. Lucas, D. K. Perkins, and T. W. van Doren, J. Acoust. Soc. Am. **104**, 623 (1998).
7. Y. A. Ilinskii, B. Lipkens, T. S. Lucas, T. W. van Doren, and E. A. Zabolotskaya, J. Acoust. Soc. Am. **104**, 2664 (1998).
8. V. F. Kovalev and O. V. Rudenko, Acoust. Phys. **58**, 269 (2012).
9. M. L. Munjal, *Acoustics of Ducts and Mufflers with Application to Exhaust and Ventilation System Design* (Wiley, New York, 1987).
10. L. L. Beranek, *Acoustical Measurements* (Wiley, New York, 1998).